Research Square

Preprints are preliminary reports that have not undergone peer review.
They should not be considered conclusive, used to inform clinical practice,
or referenced by the media as validated information.

Mechanistic Evaluation of Zinc Oxide Phyto-Nanoparticles in MDA-MB-231 Cells: Linking Cytotoxicity, Cell cycle Arrest, Apoptosis, and Caspase3 and p53 Gene Modulation

Varun Bharadwaj
JSS Science and Technology University
Aishwarya Shivashankarappa
JSS Science and Technology University
Kavitha Hunumanahalli Shankarappa
Sanjay Konasur Rajesh
sanjayrajesh@jssstuniv.in

JSS Science and Technology University

Research Article

Keywords: Anticancer, Apoptosis, Gene expression, Flow cytometry and Zinc Oxide Nanoparticles, MDA-MB-231

Posted Date: September 15th, 2026

DOI: https://doi.org/10.21203/rs.3.rs-10883829/v1

License: This work is licensed under a Creative Commons Attribution 4.0 International License.
Read Full License

Additional Declarations: No competing interests reported.

Mechanistic Evaluation of Zinc Oxide Phyto-Nanoparticles in MDA-MB-231 Cells: Linking Cytotoxicity, Cell cycle Arrest, Apoptosis, and Caspase3 and p53 Gene Modulation

First Author: Varun Bharadwaj M (varunbharadwaj@jssstuniv.in)

Affiliation: Research Scholar, JSS Science and Technology University (Department of Biotechnology), Mysuru, (Karnataka), India.

First Author and Co-Corresponding Author: Dr Aishwarya Shivashankarappa (aishwaryas@jssstuniv.in)

Affiliation: Assistant Professor, JSS Science and Technology University (Department of Biotechnology), Mysuru, (Karnataka), India.

Second Author: Kavitha Hunumanahalli Shankarappa (drkavithamph@gmail.com)

Affiliation: District Surveillance Unit, District Family Health and Welfare Office, Mysuru, India

Corresponding Author: Dr Sanjay Konasur Rajesh (sanjayrajesh@jssstuniv.in)

Affiliation: Professor, JSS Science and Technology University (Department of Biotechnology), Mysuru, (Karnataka), India.

ORCID DETAILS

Dr Aishwarya Shivashankarappa: 0000-0002-1341-0370

Dr K R Sanjay: 0000-0002-0893-5375

Abstract

Zinc oxide nanoparticles (ZnONPs) have gained considerable attention as potential nanotherapeutic agents due to their ability to modulate cellular pathways involved in tumour progression. In the present study, ZnONPs were biosynthesized using *Azadirachta indica* (Neem) and physicochemically characterized. Their anticancer activity was evaluated against the human breast cancer cell line MDA-MB-231. Cytotoxicity was assessed using the MTT assay, while cell cycle progression and apoptosis were investigated by flow cytometry using propidium iodide (PI) and Annexin V-FITC staining, respectively. Cell migration was evaluated using a cell migration assay. The molecular mechanism of ZnONP mediated cytotoxicity was investigated by quantitative PCR analysis of Caspase 3 and p53, followed by western blotting. ZnONPs exhibited pronounced cytotoxicity, producing 88.92% inhibition of cell viability at 10 µg/mL, compared with 77.60% for doxorubicin at 10 µM. Flow-cytometric analysis revealed cell cycle arrest with accumulation of cells in the G0/G1 and G2/M phases. ZnONPs also induced apoptosis, reducing viable cells to 22.33% and increasing early apoptotic cells to 31.88%. Wound closure decreased from 93.48% in controls to 58.49% following ZnONP treatment, compared with 37.81% for doxorubicin. ZnONPs significantly upregulated Caspase-3 (2.48-fold) and p53 (1.56-fold) expression. Western blot further confirmed increased Caspase 3 levels in Doxorubicin (3.25 fold) and ZnONPS (2.95 fold) and p53 levels in Doxorubicin (1.8 fold) and ZnONPs (1.66 fold) treated cells. Collectively, these findings demonstrate that green synthesized ZnONPs suppress MDA-MB-231 cell proliferation through cell cycle arrest, apoptosis induction, and inhibition of cell migration, supporting their potential as candidates for breast cancer nanotherapeutics.

Keywords: Anticancer, Apoptosis, Gene expression, Flow cytometry and Zinc Oxide Nanoparticles, MDA-MB-231

1.0 Introduction

Nanoparticles (NPs) have emerged as promising tools in cancer diagnosis and treatment [1]. Compared with conventional therapeutic approaches, NPs offer several advantages, including improved drug delivery efficiency, enhanced targeting capability, and reduced systemic side effects [2]. Their versatility allows them to be engineered for targeted therapy in different types of cancers [3]. Furthermore, nanoparticle systems can be designed to respond to tumor-specific conditions, such as the acidic microenvironment and interactions with intra and extracellular proteins [4]. Drugs can also be incorporated into nanometric matrices that regulate controlled release, thereby improving pharmacodynamic properties [5].

ZnONPs have been widely reported to exhibit significant antiproliferative activity against various cancer cell lines, including human neuroblastoma [6], epidermoid carcinoma [7], cervical cancer [8], gastric cancer [9], and breast cancer [10]. Recent research has also focused on integrating plant extracts and bioactive compounds of biological origin with anticancer potential into nanoparticle formulations, thereby expanding their biomedical applications [11,12]. ZnONPs have been reported to induce multiple cellular toxicity mechanisms in different cell types. ZnONPs trigger intracellular Ca^{2+} flux, reduce mitochondrial membrane potential, and cause loss of membrane integrity in BEAS-2B cells and RAW264.7 murine macrophages [13]. Cellular uptake studies indicate that ZnONPs enter BEAS-2B cells through caveolae-mediated endocytosis, whereas in RAW264.7 macrophages they accumulate primarily in lysosomes. Additionally, iron-doped ZnONPs exhibit reduced Zn^{2+} dissolution rates and lower cytotoxicity compared with pure ZnO nanoparticles. In A549 lung epithelial cells, ZnONPs have been shown to decrease mitochondrial activity, damage cell membranes, and stimulate the production of interleukin-8 (IL-8) and reactive oxygen species (ROS). Furthermore, ZnONPs exposure induces time and concentration dependent cytotoxicity in BEAS-2B cells, accompanied by increased lactate dehydrogenase (LDH) release, oxidative stress, elevated intracellular Ca^{2+} levels, and activation of the p53 signaling pathway [13]. ZnONPs have also been reported to stimulate IL-8 mRNA expression in both primary human bronchial epithelial cells and BEAS-2B cells [15]. Green synthesis represents an eco friendly approach for the fabrication of metallic nanoparticles by utilizing plant-derived reducing and stabilizing agents. These agents are rich in phenolic compounds and other phytochemicals containing hydroxyl groups that facilitate nanoparticle formation [10,16]. Additionally, several studies have reported that the bioactive properties of plant-derived compounds can be enhanced when incorporated into nanometric matrices [18]. Therefore, the present study evaluated the anticancer potential of plant mediated ZnONPs nanoparticles synthesized using the crude extract of *Azadirachtaindica* (Neem). The results demonstrated that these ZnONPs exhibit significant antiproliferative effects against Human breast cancer cell line MDA-MB-231 (ATCC-HTB-26). Furthermore, the nanoparticles inhibited colony formation and promoted apoptosis mediated cell death in MDA-MB-231breast cancer cells.

2.0 Materials and Methods:

2.1 Synthesis of ZnONPs

Azadirachtaindica (Neem) leaves were collected from the campus SJCE, Mysore, India. The freshly collected leaves were washed thoroughly 2-3 times with tap water to remove dust and impurities. The cleaned leaves were then chopped into small pieces and spread on aluminium foil to dry under shade for 2-3 days. After complete drying, the leaves were ground into a coarse powder. Approximately 20 g of the powdered plant material was

mixed with 500 mL of distilled water and heated with continuous stirring at 50-60 °C for 1 hour to prepare the plant extract. The mixture was then allowed to cool to room temperature and filtered using Whatman filter paper to obtain a clear filtrate. 1 mM Zinc nitrate solution was added drop wise to the filtrate while continuously stirring at 50 °C. The gradual change in colour to brownish black indicated the formation of ZnONPs. The synthesized nanoparticles were purified by centrifugation at 7000 rpm for 20 minutes. The collected precipitate was then dried in a hot air oven for 24 hours. Further purification and crystallization were achieved through calcination in a muffle furnace at 500 °C for 3 hours under limited air supply. Finally, the obtained ZnONPs were ground using a mortar and pestle to obtain uniformly sized nanoparticle powder and subjected to physio-chemical characterization (Not reported in this paper) .

2.2 Cell culture and cytotoxicity assay

Human breast cancer cell line MDA-MB-231 cell lines were obtained from the American Type Culture Collection (ATCC). The stock cells were cultured in Dulbecco's Modified Eagle Medium (DMEM) medium supplemented with 10% heat-inactivated fetal bovine serum (FBS), penicillin (100 IU/mL), and streptomycin (100 µg/mL). Cells were maintained in humidified incubator with 5% CO_2 at 37 °C until confluent [19, 20,21]. Cell viability was assessed and single cell suspension containing 5.0×10^5 cells/mL was prepared. Standard anticancer drug Doxorubicin was prepared in the concentrations ranging from 3.125, 6.25, 12.5, 25, 540 and 100 µM and ZnONPs and neem leaf powder in the concentrations ranging from 5, 10, 20, 40, 80, 160, 320 µg/mL was prepared. 100 µL of the cell suspension was seeded into each well of a 96 well microtiter plate and incubated at 37 °C in 5% CO_2 for 24 h. Following incubation, the supernatant was removed and the cell monolayer was rinsed with fresh medium. Subsequently, 100 µL of ZnONPs at different concentrations were added to the designated wells and incubated for 24 h. Following treatment, the test solutions were discarded and 100 µL of MTT reagent was added to each well. The plates were incubated for 4 h at 37 °C in 5% CO_2. The supernatant was removed and 100 µL of DMSO was added to dissolve the formazan crystals and absorbance was measured at 590 nm using a multimode microplate reader (SpectraMax i3X, Molecular Devices). The percentage of cell inhibition and IC_{50} values were determined from dose response curves using GraphPad Prism version 5.0.

2.3 Cell cycle Arrest analysis of MDA-MB-231 by flow cytometry

The human breast cancer cell line MDA-MB-231 was procured from the American Type Culture Collection (American Type Culture Collection). The cells were cultured in Dulbecco's Modified Eagle Medium (DMEM) supplemented with 10% heat-inactivated fetal bovine serum (FBS), penicillin (100 IU/mL), and streptomycin (100 µg/mL). Cells were maintained in a humidified incubator containing 5% CO_2 at 37 °C until confluent. 1×10^6 cells were seeded into a 6-well plate containing 2 mL of complete medium and incubated for 24 h at 37 °C in 5% CO_2 incubator [19, 20,21]. Standard Doxorubicin concentration of 10 µM. ZnONPs in the concentration of 5 and 10 µg/mL and neem leaf powder in the concentration of 80 and 160 µg/mL were used for treatment and incubated for 24 h. The cells were harvested by centrifuging at 2000 rpm for 5 min at room temperature and the supernatant was carefully discarded while retaining the cell pellet. The pellet was washed and resuspended in 2 mL of 1x PBS and centrifuged again to remove the supernatant. Cells were fixed by resuspending the pellet in 300 µL of sheath fluid followed by the drop wise addition of 1 mL chilled 70% ethanol with gentle vortexing.

The fixed cells were stored at 4 °C overnight. Following fixation, the cells were centrifuged at 2000 rpm for 5 min and the pellets were washed twice with 2 mL cold 1x PBS and resuspended in 450 µL sheath fluid containing propidium iodide (PI) (0.05 mg/mL) and RNase A (0.05 mg/mL) and incubated for 15 min in the dark. Cell cycle distribution was analyzed using the BD FACSLyric Flow Cytometer (BD Biosciences, San Jose, CA, USA). A total of 10,000 events were acquired for each sample, and the percentage of cells in different phases of the cell cycle (G0/G1, S, and G2/M) was determined by gating the events using PI-area versus width parameters.

2.4 Apoptosis detection using Propidium Iodide (PI) and Annexin V-fitc staining of MDA-MB-231 cells by flow cytometry

24 h prior to induction of apoptosis, 1×10^6 of MDA-MB-231 cells/well was plated in a 6 well plate using DMEM media with 10% FBS and 1% penicillin and streptomycin and incubated overnight at 37˚C at 5% CO_2. The media was replaced with standard Doxorubicin concentration of 10 µM. ZnONPs concentration of 5 and 10 µg/mL and neem leaf powder in the concentration of 80 and 160 µg/mL along with 10% FBS. The treated cells were incubated for 24 h at normal culture conditions. The cells were harvested and well contents were completely transferred to the sterile Fluorescence Activated Cell Sorting (FACS) tubes and centrifuged at 2000 rpm for 5 min and supernatant was discarded. Cells were washed twice with cold PBS following centrifugation and resuspended in 1 mL 1x binding buffer at a concentration of ~1 x 10^6 cells/mL. Cell suspension of 500 µL was transferred (~5 x 10^5 cells) to a new FACS tube and 5 µLof Annexin V and 10 µL PI was added to the tubes, cells were gently mixed and incubated for 15 min at room temperature in a dark condition and analysed by flow cytometry immediately [22].

2.5 Wound Healing Assay

Cells were detached by trypsinization using 0.25% trypsin and EDTA solution. The cells were centrifuges and the supernatant was resuspended in culture media (DMEM). 10^5 cells were plated in a 6 well plate and 100% confluent cells were picked for analysis. With a help of 200µl micro pipette tip, a 2 mm scratch was made swiftly on top of the tissue culture plate through the cell monolayer. The cell debris were carefully removed and enough media was added against the walls of the well to avoid detachment of any other cells. Initial observation was noted and the plates were incubated at 37^0 C with 5% CO_2. For every 24 h, image was captured under an inverted microscope to assess the migration of the cells and the distance from the point of wound was measured on both sides using ImageJ software.

The wound closure was calculated in percentage using the formula:

$$Wound\ Closure\ (\%) = \frac{Migration\ distance\ at\ 0\ h - Migration\ distance\ at\ time\ 't'}{Migration\ distance\ at\ 0\ h} \times 100$$

2.6 Gene expression study of Caspase 3 and P53 gene using MDA-MB-231

Cells density at 1×10^6 cells/mL were added to culture medium and incubated for 24 h at 37 °C in a humidified atmosphere containing 5% CO_2. Following incubation, the culture medium was carefully removed and the cells

were treated with doxorubicin of 10 µM concentration, ZnONPs at concentrations of 5 µg/mL and 10 µg/mL, and neem leaf extract at concentrations of 80 µg/mL and 160 µg/mL. The treated cells were further incubated for 24 h at 37 °C in a CO_2 incubator.

2.61 RNA Isolation

Cells were dissociated, rinsed with sterile 1X PBS, and centrifuged. The supernatant was discarded and 0.4 mL of TRIzol reagent was added and mixed gently. The samples were added with 0.25 mL chloroform per 0.4 mL of TRIzol and incubated at room temperature for 5 min. The samples were then centrifuged at 12,000 rpm for 15 min at 4 °C. The upper aqueous phase was carefully transferred to a new sterile microcentrifuge tube, and 0.5 mL of isopropanol was added. The mixture was incubated at -20 °C for 20 min and subsequently, centrifuged at 12,000 rpm for 10 min at 4 °C. The supernatant was discarded and the RNA pellet was washed with 70% ethanol, followed by centrifugation at 12,000 rpm at 4 °C [23]. The supernatant was carefully removed and the pellet was air dried and resuspended in 20 µL of Diethyl pyrocarbonate (DEPC) treated water, and the total RNA concentration was quantified using Spectra Drop (SpectraMax i3x, Molecular Devices, USA).

2.62 cDNA synthesis

The cDNA was synthesized from 500 ng of RNA using the cDNA synthesis kit from Prime script RT reagent kit (TAKARA) with oligo dT primer. The reaction volume was set to 20µl and cDNA synthesis was performed at 50ºC for 30min, followed by RT inactivation at 85ºC for 5 min using applied biosystems, Veritii. The cDNA was further used for real time PCR analysis. The PCR mixture (final volume of 20 µl) contained 1.4 µl of cDNA, 10 µL of SyBr green master mix and 1 µM of complementary forward and reverse primers specific for GAPDH, Caspase 3 and p53 genes. The reaction was carried out with enzyme activation at 95ºC for 2 minutes followed by two step reaction with initial denaturation, annealing and extension at 95°C for 5 seconds, annealing for 30 seconds was given at specific temperature for all 3 genes and amplified for 39 cycles followed by secondary denaturation at 95 °C for 5 seconds. One cycle melt curve analysis was done at temperature from 65°C to 95°C for 5 seconds each [23]. The obtained results were analysed to calculate the fold expression of gene regulation.

2.7 Protein Expression of Caspase 3 and p53 by SDS PAGE and Western blotting

Cells treated with doxorubicin, ZnONPs and neem extract were harvested and washed with 1X PBS. The cells were gently suspended in 300 µl Radioimmunoprecipitation assay buffer (RIPA) buffer with protease inhibitor. The cells were incubated for 30 min at 4^0 C with intermittent mixing every 5 mins once and centrifuged at 10,000 RPM for 15 mins. The protein lysates in the supernatant was collected for further analysis.

For SDS PAGE, the protein concentration was quantified and 25 µg protein was mixed with 5X loading dye and heated for 2 min at 95^0 C. The SDS PAGE separation of protein was done using three different gels (8%, 10% and 15%) using Mini Protean Tetra Cell, Bio-Rad. 0.2 µm nitrocellulose membrane was equilibrated with a transfer buffer for 10 mins at room temperature (RT). The protein transfer was done for 15 min in Turbo Transblot, Bio-Rad at 2.5 A and 25 V. The blot was blocked using 3% BSA Tris Buffer Saline with Tween (TBST) for 1 hour and subsequently treated with primary antibodies against caspase-3 (31 kDa) and p53 (53 kDa) overnight at 4^0 C and GAPDH (36 kDa) was used as the loading control. Following incubation, the blot was washed three times with TBST at room temperature and treated with Peroxidase AffiniPure® Goat Anti-

Rabbit IgG [H+L] secondary antibody for 1 hour at RT. The blot was again washed with TBST and developed using two component with Enhanced Chemiluminescence Regent (ECL) for 1 min in dark and image was captured between 0.5 sec to 15 secs exposure in Chemidoc XRS+ imaging system (Bio-Rad).

Caspase 3 and p53 expression was normalized against the house keeping gene GAPDH to check for any variations in the expression levels. The normalized expression was calculated by the formula

$$Normalized\ Protein\ expression\ = \frac{Band\ Intensity\ of\ the\ Test}{GAPDH\ Band\ Intensity}$$

The normalized value of the untreated sample was assigned a fold regulation of 1.0 and the fold regulation of each sample was calculated and compared relative to the the control using the formula

$$Fold\ Regulation\ = \frac{Normalized\ Value\ of\ Treatment}{Normalized\ Value\ of\ Control}$$

3.0 Results

3.1 Cytotoxicity studies Cell Cycle Study on MDA-MB-231 cells using Flow Cytometer

The MDA-MB-231 cells treated with neem leaf extracts and ZnONPs exhibited dose dependent inhibition of cancer cell (Fig 2)**.** The standard Doxorubicin at a concentration of 10 µM exhibited an inhibition of 76.66% with an IC_{50} of 15.99 µg/mL (Fig 1a) while the ZnONPs at a concentration of 320 µg/mL showed an inhibition of 88.92% with an IC_{50} value of 37.9 µg/mL. The neem leaf extracts exhibited comparatively low cytotoxicity when compared to standard and ZnONPs treated cells with an inhibition of 52% and an IC_{50} value of 307.6 µg/mL (Fig 1b).

3.2 Cell Cycle Arrest analysis of MDA-MB-231

The results on cell cycle arrest indicated that control group had maximum 58.86% cells in G0/G1 phase, 9.43% in the S phase, and 18.55% in the G2/M phase. This indicated that the majority of cells were in the resting or quiescent stage (G0/G1), while a relatively smaller population of cells was actively progressing through DNA synthesis and mitosis (S and G2/M phases). The positive control, doxorubicin treated cells, exhibited 29.43% of cells in the G0/G1 phase, 8.2% in the S phase, and 25.88% in the G2/M phase. Compared to the control group, doxorubicin treatment resulted in a marked reduction in the G0/G1 population and an increase in the G2/M phase, suggesting cell cycle arrest predominantly at the G2/M phase. Treatment with Neem extract demonstrated a dose-dependent effect on cell cycle progression. At 160 µg/mL, 50.63% of cells were observed in G0/G1 phase, 8.68% cells in S phase and 20.52% cells in G2/M phase indicating a possible G2 phase arrest induced by Neem extract. ZnONPs similarly exhibited a dose-dependent influence on cell cycle distribution. At 10 µg/mL, 39.62% of cells were observed in the G0/G1 phase, 5.71% in S phase and 19.95% cells in G2/M phase (Fig 3a). These results indicate cellular stress and DNA damage caused by the ZnONPs. This arrest prevents the cell from further undergoing mitosis followed by apoptosis. One way ANAOVA was performed to compare the all the test samples with control which indicated that there was a significant different with control compared with standard drug and ZnONPs with a $p<0.0001$ which indicated that the ZnoNPs and doxorubicin had deleterious effect on the DNA of the cells. The ZnoNPs were comparable to standard drug doxorubicin

indicating that high accumulation of cells in G2/M phase than in G0/G1 and S phase exerting anticancer activity partly through modulation of cell cycle progression and subsequent induction of apoptosis (Fig 3b).

3.3 Apoptosis detection using PI and Annexin V-FITC staining of MDA-MB-231 cells by flow cytometry

The result of apoptosis analysis using PI and Annexin V–FITC (Annexin V - Fluorescein isothiocyanate) by flow cytometry on MDA-MB-231 cells is shown in Fig 4a. The control showed 76.59% viable cells, 5.95% early apoptotic cells, 0.53% late apoptotic cells, and 0.55% necrotic cells, which served as the baseline for comparison. The positive control showed a marked induction of apoptosis with only 11.78% viable cells, while early apoptosis increased to 46.47%, late apoptosis to 1.46%, and necrosis was 0.18%. This indicates the strong apoptosis inducing capability of the standard drug. Treatment with Neem extract at 80 µg/mL slightly reduced the percentage of viable cells (69.09%) compared to the control, with a minor increase in early apoptosis (3.22%), along with small increases in late apoptosis (1.46%) and necrosis (0.18%). When the concentration was increased to 160 µg/mL, a further reduction in viable cells (68.01%) was observed, accompanied by a slight rise in early apoptosis (3.61%), a more noticeable increase in late apoptosis (7.17%), and necrosis (5.13%). These results suggest that neem extract induces apoptosis and necrosis in a concentration dependent manner, although the effect is less pronounced compared to the standard drug. ZnONPs showed a stronger apoptotic effect, at 5 µg/mL, the percentage of viable cells decreased to 27.24%, while early apoptosis significantly increased to 31.76%, with minimal changes in late apoptosis (0.48%) and necrosis (0.56%). Increasing the concentration to 10 µg/mL further reduced viable cells to 22.33%, while early apoptosis remained relatively similar (31.88%), with slight increases in late apoptosis (1.23%) and a decrease in necrosis (0.24%) (Fig 4b). These findings indicate that ZnONPs effectively induce apoptosis in MDA-MB-231 cells, predominantly through early apoptotic pathways, suggesting their potential cytotoxic and anticancer activity.

3.4 Cell Migration Assay

The cell migration assay demonstrated a strong inhibitory effect of the test sample on cellular migratory ability when compared with the control. While the untreated cells exhibited a 68.59% migration at 24 hours and increased to 93.94% at 48 h showing an increased wound healing activity with increasing incubation time, the ZnONPs at 10 µg exhibited a stronger antimigratory activity reducing the wound closure to 15.33% at 24 h and 58.49% at 48 h. The neem extract had comparatively lower antimigratory activity than ZnONPs with a reduced wound closure of 43.00% at 24 h and 78.90% at 48 h. The Doxorubicin showed the highest inhibitory activity with a drastic reduction in wound closure to 9.15% at 24 h and 37.81% at 48 h. Table 1 shows comparison of untreated group with ZnONPs which inhibited migration by 77.65% at 25 h and 37.74% at 48 h, while Doxorubicin inhibited migration by 88.66% at 24 h and 59.75% at 48 h (Fig 5). The statistical analysis by two way ANOVA comparing the test samples with control indicated that ZnoNPS had a significant reduction in migration with $P<0.0001$****

3.5 Gene Expression study of Caspase 3 and P53 gene using Breast cancer cells (MDA-MB-231)

The RT-PCR analysis of the target genes Caspase-3 and p53 in MDA-MB-231 cells was performed and fold regulation was determined in comparison to control cells. The cells treated with Doxorubicin showed an up-

regulation of Caspase 3 gene level with an appreciable 3.09 fold increase at a concentration of 10 µM, while ZnONPs showed a 2.48 fold increase at a concentration of 10 µg/mL and 1.38 fold increase at a concentration of 5 µg/mL. The cells treated with neem extract exhibited 1.29 fold increase at a concentration of 160 µg/mL and 1.10 fold increase at a concentration of 80 µg/mL. (Table 2) The statistical analysis performed by one way ANOVA indicated that there was significant difference between the control group and the ZnONPs treated samples with a P <0.0001 (Fig 6). The expression of p53 in doxorubicin treated cells also showed an up-regulation with 2.25 fold increase in gene level at a concentration of 10 µM, while the ZnONPs treated sample showed a slightly decrease in the gene level compared to standard drug with 1.56 fold increase at 10 µg/mL and 1.13 fold increase at 5µg/mL. Treatment with neem extract did not show much change and indicated a 1.37 fold and 1.11 fold increase in gene levels at 160 µg/mL and 80 µg/mL respectively (Table 3). The one way ANOVA test indicated that there was significant difference between the control and standard drug and ZnONPS treated sample with value P <0.0001 (Fig 7). Overall, the results indicate that ZnONPs induced a stronger up-regulation of apoptosis related genes compared to neem extract, suggesting their potential role in promoting apoptotic pathways in MDA-MB-231 breast cancer cells.

3.6 Protein Expression of Caspase 3 and p53 by SDS PAGE and Western Blotting

Western blot analysis demonstrated a steep increase in the expression of Caspase 3 and p53 proteins with the in cells treated with doxorubicin and ZnONPs. The doxorubicin treated cells showed a 3.25 fold increase in the levels of Caspase 3 with a normalized value of 0.82 compared with a control value of 0.26. The p53 levels also showed a considerable 1.8 fold increase with a noramalized value of 4.50 compared with a control value of 2.40. The ZnoNPS treated samples indicated that there was a significant 2.95 fold increase in the expression of Caspase 3 from 0.26 in untreated to 0.76 in 10 µg/mL ZnONPs treated cells. The p53 expression showed a 1.66 fold increase in the expression level with untreated control showing a normalized value of 2.40 while the cells treated with 10 µg/mL ZnONPs had a value of 3.98. However, the neem extract did not have a significant effect on the expression levels and displayed 0.83 fold increase in Caspase 3 levels and 0.78 fold increase in p53 levels indicating that neem extracts were not highly effective under the given condition (Fig 8).

4.0 Discussion

In the present study, the potential cytotoxic effects of zinc oxide nanoparticles (ZnONPs) were evaluated and the mechanism of action of nanoparticles was studied through various evaluations like cell cycle arrest, apoptosis induction, cell migration and expression of apoptosis related genes which indicated that the zinc oxide nanoparticles exhibit cytotoxicity through various intermolecular mechanisms. The cytotoxicity assay revealed a dose dependent reduction in the viability of cells following treatment with both neem extract and ZnONPs. The lower IC_{50} value obtained for doxorubicin (15.99 µg/mL) confirms the established potency as a chemotherapeutic agent. But however, ZnONPs exhibited a considerably stronger cytotoxic effect than the crude neem extract, achieving 88.92% growth inhibition. The enhanced cytotoxicity of ZnONPs can be attributed to nanoscale properties like increased surface area, improved cellular internalization and physico chemical interaction, generation of reactive oxygen species (ROS) [24]. A study conducted by Aishwarya et.al 2022, also confirmed that the production of ROS molecules due to absorption of light enhances the cytotoxicity of the nanoparticles [25]. Cell cycle arrest determined by flow cytometric analysis further demonstrated that both

standard drug doxorubicin and ZnONPs have the potential to interfere with the cell cycle regulation. In the untreated control cells it was observed that the cells predominantly remained in the G0/G1 phase reflecting the normal growth and proliferation cycle. However, in the doxorubicin treatment, the cells were significantly concentrated in the G2/M phase, reducing the population in G0/G1 confirming the induction of DNA damage and activation of G2/M checkpoint. Similar results were seen in cells treated with ZnONPs where there was marked shift in the concentration of cells in G0/G1 phase and accumulation in G2/M phase [26]. This indicates the activation of G2/M checkpoint following extreme exposure to nanoparticles. DNA damage triggers the ATM/ATR signalling pathways, which subsequently phosphorylate the kinases (Chk1 and Chk2), leading to inhibition of cyclin B/CDK1 complexes and halts the cell progression at G2/M phase. This arrest prevents damaged cells from entering mitosis and serves as an important protective mechanism before apoptosis is initiated [26, 27]. In contrast to ZnONPs, the neem extract did not show much change and although a slight increase in G2/M phase cells was observed with increasing concentration, the majority of cells remained in the G0/G1 phase, suggesting limited interference with cell cycle progression due to the limited intracellular uptake and bioavailability compared to nanoparticles [28]. The Annexin V-FITC/PI apoptosis assay confirmed that the inhibition of cell cycle was primarily associated with the G2/M phase induction of programmed cell death rather than non specific necrosis. The control cells exhibited viable population with minimal apoptotic cells. Doxorubicin treated cells showed a significant reduction in the viable cells accompanied by increase in early apoptotic cells validating that the drug had effectively activated the apoptotic mechanism. ZnONPs demonstrated a prominent apoptotic response even at low concentration declining the viable cell count and indicating a predominant mechanism of cell death. The presence of relatively low percentage of necrotic cells indicates that nanoparticles activated a regulated apoptotic pathway and had not caused extensive membrane disruption or uncontrolled cytotoxicity [29, 30, 31]. The cells treated with neem extract demonstrated a gradual decrease in viable cells indicating late apoptosis and necrosis. The migration assay revealed that ZnONPs were able to efficiently inhibit the migratory capacity of the MDA-MB-231 cells. Although there was a slight increase in the migration from 24 h to 48 h (15.33% to 58.49%), the overall wound closure remained comparatively lower than untreated cells. Similar results were observed by a study conducted by Esnaashari et al, 2025 and Yu et al, 2025 on treating breast cancer cell line MCF-7 with zinc oxide loaded chitosan nanoparticles and ZnO nanoparticles which showed there was up regulation of Caspase 8 & 9 along with Claudin -2 while there was a significant decrease in the migration activity of the cells in both studies [32, 33]. The stronger inhibition observed in ZnONPs compare to neem extract may be due to enhanced biological activity of nanoparticles and their efficient interaction with cancer cells. The surface associated phytochemicals may have played a crucial role in their biological activity and cellular uptake [34]. Notably, the ZnONPs approached near values to standard drug Doxorubicin at 24 h indicating a reduction in the overall wound healing capacity. The real time PCR analysis of standard doxorubicin exhibited highest fold increase in caspase 3 levels while ZnONPs produced substantially greater fold increase when compared with neem extract indicating the activation of apoptotic signalling pathway. The statistically significant differences observed by one-way ANOVA ($P < 0.0001$) further confirmed that the increased expression is unlikely to have occurred by chance. Elevated Caspase-3 expression strongly correlates with the increased proportion of Annexin V-positive apoptotic cells observed during flow cytometric analysis [35, 36]. Similar results were observed in the expression of p53 gene levels. The p53 functions as a central regulator of cellular response to DNA damage. It either promotes the

repair mechanism or initiates apoptosis depending on the extent of DNA damage. Up regulation in p53 post ZnONPs treatment indicates activation of apoptosis pathway which is consistent with the results of G2/M arrest. This mechanism promotes the pro apoptotic genes like Bax and suppress the anti apoptotic proteins like Bcl-2 leading to mitochondrial membrane permeabilization and Caspase 3 activation [37, 38, 39]. The cytotoxicity, apoptosis and gene expression clearly indicates a sequential mechanism of ZnONPs mediated anti cancer activity. Initially ZnONPs are believed to enter breast cancer cells and generate intracellular oxidative stress through the production of ROS molecules. The ROS induced DNA damage activates the p53 dependent checkpoint at G2/M phase. However due to extreme ROS exposure, the DNA repair mechanism fails and mitochondrial apoptotic pathways gets activated leading to Caspase 3 activation and ultimately leading to cell death [40, 41]. This co-ordinated molecular sequence of events explains the observed reduction in the viability of the cells and enhanced apoptosis. Western blot assay showed increased levels of Caspase 3 and p53 in both doxorubicin and ZnONPs treated cells indicating the role of caspase in terminal stages of apoptosis, which supports the increased action of apoptosis in the present study [42, 43]. The neem extract had limited change in the expression levels of Caspase 3 and p53 indicating a weaker induction of apoptosis markers which may also be the reason for its low activity on wound closure which may be due to insufficient exposure to phytochemicals or experimental conditions. Overall, the study demonstrates that zinc oxide nanoparticles induce anti migratory and apoptotic effects against MDA-MB-231 cells. The significant reduction on the wound healing capacity along with increased expression of Caspase 3 and p53 suggest that nanoparticles interfere with cancer cells progression along with suppression of wound healing and trigger the apoptotic signalling pathway. The superior biological activity of ZnONPs proved to have improved cellular uptake through endocytosis, intracellular retention which increases the oxidative stress and subsequently triggers apoptotic mechanism by systemic toxicity associated with conventional chemotherapy. Though Doxorubicin performed better, the ability of the ZnONPs to substantially inhibit cancer cell progression make them a potential candidate as plant mediated nanotherapeutic agents for evaluation on cancer models.

5.0 Conclusion

The present study demonstrated that green synthesized ZnO nanoparticles excellent anticancer activity against MDA-MB-231 breast cancer cells. It was found that ZnONPs induced dose dependent cytotoxicity, promoted G2/M phase cell cycle arrest, enhanced apoptosis largely through early apoptotic pathway, reduced wound closure and appreciably up regulated the expression of the apoptotic genes Caspase-3 and p53. These findings suggest that ZnONPs inhibit breast cancer cell proliferation by activating DNA damage mediated apoptotic pathways and may serve as a promising, biocompatible nanotherapeutic candidate for the treatment of triple negative breast cancer. Further scope of work could be focused on in vivo studies and molecular investigations to validate their clinical applicability and safety.

6.0 Acknowledgements

The authors like to thank the JSS Mahavidyapeetha for providing opportunity to work in their institution. The authors also express gratitude to JSS Science and technology University, Department of Biotechnology for the facilities and infrastructure.

7.0 Declaration of Interest

The authors declare that they have no known competing financial interests or personal relationships that could have appeared to influence the work reported in this manuscript.

8.0 Funding Declaration

The authors declare that there was no funding provided by any government bodies or private institutions for the present work.

9.0 Disclosure Statement

The authors confirm that there is no financial or non-financial interest that is linked to the present work in any form.

10.0 Data Availability Statement

All the data which is relevant to the work are provided in the manuscript, if there is any other information required will be provided on request.

8.0 Reference

1. Sakahashi, Y., Higashisaka, K., Isaka, R., Izutani, R., Seo, J., Furuta, A., Yamaki-Ushijima, A., Tsujino, H., Haga, Y., Nakashima, A., &Tsutsumi, Y. (2022). Silver nanoparticles suppress forskolin-induced syncytialization in BeWo cells. Nanotoxicology, 16(9–10): 883–894. https://doi.org/10.1080/17435390.2022.2162994

2. Raj, S., Khurana, S., Choudhari, R., Kesari, K. K., Kamal, M. A., Garg, N., Ruokolainen, J., Das, B. C., & Kumar, D. (2019). Specific targeting cancer cells with nanoparticles and drug delivery in cancer therapy. Seminars in Cancer Biology, 69. https://doi.org/10.1016/j.semcancer.2019.11.002.

3. Surya, C., Lakshminarayana, A. B. V., Ramesh, S. H., Kunjiappan, S., Theivendren, P., Santhana Krishna Kumar, A., Ammunje, D. N., &Pavadai, P. (2024). Advancements in breast cancer therapy: The promise of copper nanoparticles. Journal of Trace Elements in Medicine and Biology : Organ of the Society for Minerals and Trace Elements (GMS), 86: 127526. https://doi.org/10.1016/j.jtemb.2024.127526

4. Nam, J.-M. (2003). Nanoparticle-Based Bio-Bar Codes for the Ultrasensitive Detection of Proteins. Science, 301(5641): 1884–1886. https://doi.org/10.1126/science.1088755

5. Holghoomi, R., Kiani, M. H., Rahdar, A., Hashemi, S. M., Romanholo Ferreira, L. F., &Fathi-karkan, S. (2024). Nanoparticle-delivered gallic acid: A new frontier in cancer therapy. Journal of Drug Delivery Science and Technology, 101: 106129. https://doi.org/10.1016/j.jddst.2024.106129

6. Kim, J.-H., Jeong, M. S., Kim, D.-Y., Her, S., & Wie, M.-B. (2015). Zinc oxide nanoparticles induce lipoxygenase-mediated apoptosis and necrosis in human neuroblastoma SH-SY5Y cells. Neurochemistry International, 90: 204–214. https://doi.org/10.1016/j.neuint.2015.09.002

7. Khan, M. J., Ahmad, A., Khan, M. A., & Siddiqui, S. (2021). Zinc Oxide Nanoparticle Induces Apoptosis in Human Epidermoid Carcinoma Cells Through Reactive Oxygen Species and DNA Degradation. Biological Trace Element Research, 199(6): 2172–2181. https://doi.org/10.1007/s12011-020-02323-4

8. Lei, J., Ploner, A., Elfström, K. M., Wang, J., Roth, A., Fang, F., Sundström, K., Dillner, J., &Sparén, P. (2020). HPV Vaccination and the Risk of Invasive Cervical Cancer. New England Journal of Medicine, 383(14): 1340–1348. https://doi.org/10.1056/nejmoa1917338

9. Du, W., Feng, K., Li, C., Li, S., Abidin, Z. U., Yin, H., & Chen, S. (2023). Controlled synthesis of zinc oxide nanoparticles through flame spray pyrolysis and evaluation of their anticancer effects against gastric cancer cell. Arabian Journal of Chemistry, 16(10): 105192. https://doi.org/10.1016/j.arabjc.2023.105192

10. Benine, C., Boutlelis, D. A., Touhami, L. A., Lanez, E., Ghemam Amara, D., Rim, G., Hanen, N., Zahnit, W., & Messaoudi, M. (2025). Green synthesis, characterization, antioxidant, interaction with DNA/BSA, and investigation of cytotoxicity against MCF-7 cancer cells of zinc oxide nanoparticles using Hammadascoparia (Pomel) Iljin extract. International Journal of Biological Macromolecules, 295: 139709. https://doi.org/10.1016/j.ijbiomac.2025.139709

11. Alvarez-Gutiérrez, P. E., Ruiz-Ramirez, L. A., Godoy-Hernández, G. C., & Gutiérrez-Miceli, F. A. (2020). Bonediol Production in Bonelliamacrocarpa Hairy Root Culture. Reference Series in Phytochemistry, 585–605. https://doi.org/10.1007/978-3-030-30185-9_24

12. Jonapá-Hernández, F., Jacobo-Herrera, N. J., del Carmen Couder-García, B., Montes-Molina, J. A., Gutiérrez-Miceli, F. A., Pérez-Arteaga, E., &Luján-Hidalgo, M. C. (2025). Cytotoxic effect of zinc oxide phytonanoparticles and Bonelliamacrocarpa (Cav.) B. Stahl &Källersjö extract on breast cancer cell lines. Journal of Materials Science: Materials in Engineering, 20(1). https://doi.org/10.1186/s40712-025-00282-z

13. George, S., Pokhrel, S., Xia, T., Gilbert, B., Ji, Z., Schowalter, M., Rosenauer, A., Damoiseaux, R., Bradley, K. A., Mädler, L., & Nel, A. E. (2009). Use of a Rapid Cytotoxicity Screening Approach To Engineer a Safer Zinc Oxide Nanoparticle through Iron Doping. ACS Nano, 4(1): 15–29. https://doi.org/10.1021/nn901503q

14. Ng KW, Khoo SP, Heng BC, Setyawati MI, Tan EC, Zhao X, Xiong S, Fang W, Leong DT, Loo JS. (2009). The role of the tumor suppressor p53 pathway in the cellular DNA damage response to zinc oxide nanoparticles. Biomaterials. 32(32): 8218–8225

15. García-López, J. I., Zavala-García, F., Olivares-Sáenz, E., Lira-Saldívar, R. H., Díaz Barriga-Castro, E., Ruiz-Torres, N. A., Ramos-Cortez, E., Vázquez-Alvarado, R., & Niño-Medina, G. (2018). Zinc Oxide Nanoparticles Boosts Phenolic Compounds and Antioxidant Activity of Capsicum annuum L. during Germination. Agronomy, 8(10): 215. https://doi.org/10.3390/agronomy8100215

16. Zhao, J., Hu, Y., Zhou, S., Li, W., Song, Z., Fan, Q., Liu, X., Meng, X., Wang, X., & Zhang, H. (2024). Evaluation of the anti-breast cancer properties of Origanummajorana aqueous extract green-mediated nanoparticles. Inorganic Chemistry Communications, 169: 113098. https://doi.org/10.1016/j.inoche.2024.113098

17. Bandeira, M., Giovanela, M., Roesch-Ely, M., Devine, D. M., & da Silva Crespo, J. (2020). Green synthesis of zinc oxide nanoparticles: A review of the synthesis methodology and mechanism of formation. Sustainable Chemistry and Pharmacy, 15: 100223. https://doi.org/10.1016/j.scp.2020.100223

18. Dousari, A. S., Hosseininasab, S. S., Akbarizadeh, M. R., Naderifar, M., &Satarzadeh, N. (2023). Mentha pulegium as a source of green synthesis of nanoparticles with antibacterial, antifungal, anticancer, and antioxidant applications. Scientia Horticulturae, 320: 112215. https://doi.org/10.1016/j.scienta.2023.112215.

19. Kumar, M. H., & P, S., & K, B. K., & Ram, A. B. (2025). A study on the anti-cancer, anti-oxidant and anti-bacterial activities of Alternanthera ficoidea (L.) R. Br against human breast cancer cells (MCF-7). International Journal of Innovative Research in Technology, 11(10): 1447–1458

20. Patil, A. B., & Shinde, A. J. (2024). Cytotoxic, apoptotic, and anti-inflammatory properties of Adenoon indicum leaf methanolic extract using HT29 cell lines. Bangladesh Journal of Pharmacology, 19(4): 122–127. https://doi.org/10.3329/bjp.v19i4.78705

21. Rajashekara, S., Konyak, M. K., Sarala, R., Poojashree, K. S., Bai, P., & Nagabhushana, J. (2025). Is sacred animal (Asian Elephant) can be a medicinal repository: a new approach for colon cancer treatment using the methanolic extracts of the dung samples and their valuation for antimicrobial, cytotoxic, and apoptotic actions. BMC Complementary Medicine and Therapies, 25(1). https://doi.org/10.1186/s12906-025-05039-x

22. Paarakh, M. P., & Ani, J. P. (2020). In vitro anticancer activity of silver nanoparticle synthesized from Punica granatum dried peel against cancer cell lines. Indian Journal of Natural Products & Resources, 11(4): 224. DOI: 10.56042/ijnpr.v11i4.29583

23. Raghavan, P. (2026). Metadichol Orchestrates T, B, and NK Cell Immunity Through Master Regulator Gene Networks. Medical Research Archives, 14(7). https://doi.org/10.18103/mra.2026.0422

24. Majeed, S., Danish, M., Ismail, M. H. Bin, Ansari, M. T., & Ibrahim, M. N. M. (2019). Anticancer and apoptotic activity of biologically synthesized zinc oxide nanoparticles against human colon cancer HCT-116 cell line- in vitro study. Sustainable Chemistry and Pharmacy, 14: 100179. https://doi.org/10.1016/j.scp.2019.100179

25. Aishwarya Shivashankarappa, K.R. Sanjay, Dhruvi Shah, Aishwarya Tagat, *Decalepis hamiltonii* derived gold nanoparticles and photodynamic cytotoxic evaluation on skin melanoma (B16F10) cells as an effective drug delivery vehicle, Journal of Drug Delivery Science and Technology, Volume 76, 2022: 103766. https://doi.org/10.1016/j.jddst.2022.103766.

26. Wilhelmi, V., Fischer, U., Weighardt, H., Schulze-Osthoff, K., Nickel, C., Stahlmecke, B., Kuhlbusch, T. A. J., Scherbart, A. M., Esser, C., Schins, R. P. F., & Albrecht, C. (2013). Zinc Oxide Nanoparticles Induce Necrosis and Apoptosis in Macrophages in a p47phox- and Nrf2-Independent Manner. PLoS ONE, 8(6): e65704. https://doi.org/10.1371/journal.pone.0065704

27. Patrón-Romero, L., Luque-Morales, P. A., Loera-Castañeda, V., Lares-Asseff, I., Leal-Ávila, M. Á., Alvelais-Palacios, J. A., Plasencia-López, I., & Almanza-Reyes, H. (2022). Mitochondrial Dysfunction Induced by Zinc Oxide Nanoparticles. Crystals, 12(8): 1089. https://doi.org/10.3390/cryst12081089

28. Condello, M., De Berardis, B., Ammendolia, M.G., Barone, F., Condello, G., Degan, P.,Meschini, S. (2016). ZnO nanoparticle tracking from uptake to genotoxic damage in human colon carcinoma cells. Toxicol. 35:169–179. https://doi.org/10.1016/j.tiv.2016.06.005

29. Wang, J., Deng, X., Zhang, F., Chen, D., & Ding, W. (2014). ZnO nanoparticle-induced oxidative stress triggers apoptosis by activating JNK signaling pathway in cultured primary astrocytes. Nanoscale Research Letters, 9(1). https://doi.org/10.1186/1556-276x-9-117

30. Shawki, M. M., El Sadieque, A., Elabd, S., &Moustafa, M. E. (2022). Synergetic Effect of Tumor Treating Fields and Zinc Oxide Nanoparticles on Cell Apoptosis and Genotoxicity of Three Different Human Cancer Cell Lines. Molecules (Basel, Switzerland), 27(14): 4384. https://doi.org/10.3390/molecules27144384

31. Cheng, J., Wang, X., Qiu, L., Li, Y., Marraiki, N., Elgorban, A. M., &Xue, L. (2020). Green synthesized zinc oxide nanoparticles regulates the apoptotic expression in bone cancer cells MG-63 cells. Journal of Photochemistry and Photobiology. B, Biology, 202: 111644.https://doi.org/10.1016/j.jphotobiol.2019.111644

32. Esnaashari, F., Zamani, H., Zahmatkesh, H., Soleimani, M., Dashtaki, G. A., & Rasti, B. (2025). Berberine decorated zinc oxide loaded chitosan nanoparticles a potent anti cancer agent against breast cancer. Scientific Reports, 15(1). https://doi.org/10.1038/s41598-025-87445-2

33. Yu, N., Hu, J., Kang, D., He, J., & Wang, M. (2025). Promotional effects of aged ZnO nanoparticles on migration, invasion and metastasis of human breast cancer MCF-7 cells in vitro and in vivo. Biochemistry and Biophysics Reports, 44: 102294. https://doi.org/10.1016/j.bbrep.2025.102294

34. Ahmed S, Ahmad M, Swami BL, Ikram S. (2016). A review on plants extract mediated synthesis of silver nanoparticles for antimicrobial applications: a green expertise. Journal of Advanced Research. 7(1):17–28. http://doi:10.1016/j.jare.2015.02.007

35. Ahamed, M., Javed Akhtar, Kumar, Khan, M., Ahmad, & Alrokayan. (2012). Zinc oxide nanoparticles selectively induce apoptosis in human cancer cells through reactive oxygen species. International Journal of Nanomedicine, 845. https://doi.org/10.2147/ijn.s29129

36. Wahab, R., Khan, F., Yang, Y., Hwang, I. H., Shin, H.-S., Ahmad, J., Dwivedi, S., Khan, S. T., Siddiqui, M. A., Saquib, Q., Musarrat, J., Al-Khedhairy, A. A., Mishra, Y. K., & Ali, B. A. (2016). Zinc oxide quantum dots: multifunctional candidates for arresting C2C12 cancer cells and their role towards caspase 3 and 7 genes. RSC Advances, 6(31): 26111–26120. https://doi.org/10.1039/c5ra25668b

37. Moselhy, O. A., Abdel-Aziz, N., El-bahkery, A., Moselhy, S. S., & Ibrahim, E. A. (2025). Curcumin nanoparticles alleviate brain mitochondrial dysfunction and cellular senescence in γ-irradiated rats. Scientific Reports, 15(1). https://doi.org/10.1038/s41598-025-87635-y

38. Shaik, M. R., Kandaswamy, K., Guru, A., Khan, H., Giri, J., Mallik, S., Shah, M. A., &Arockiaraj, J. (2024). Piperine-coated zinc oxide nanoparticles target biofilms and induce oral cancer apoptosis via BCl-2/BAX/P53 pathway. BMC Oral Health, 24(1). https://doi.org/10.1186/s12903-024-04399-z

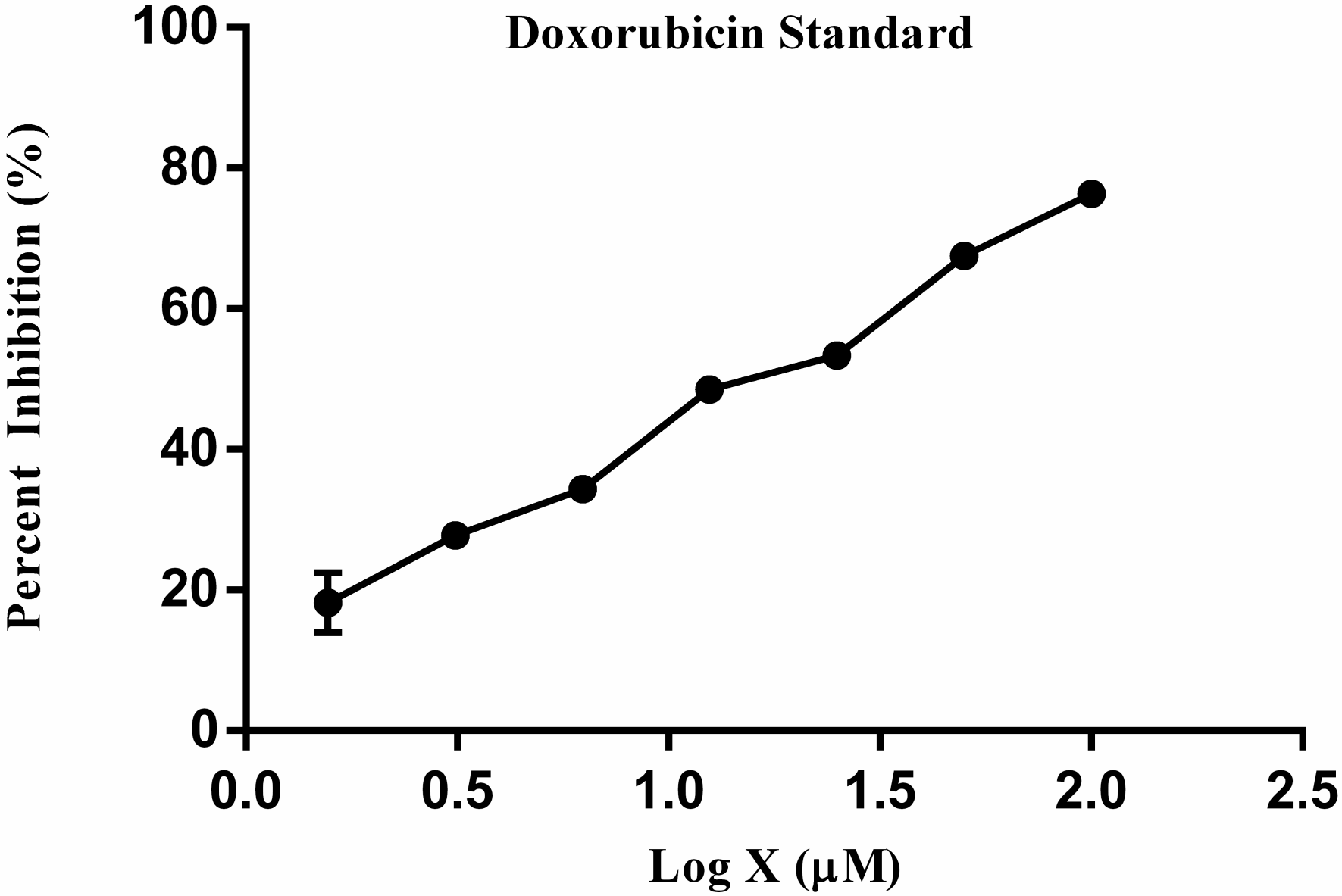
39. Zheng, X., Wang, T., Gong, J., Yang, P., Zhang, Y., Zhang, Y., Cao, N., Zhou, K., Li, Y., Hua, Y., Zhang, D., Gu, Z., & Li, Y. (2024). Biogenic derived nanoparticles modulate mitochondrial function in cardiomyocytes. Materials Horizons, 11(20): 4998–5016. https://doi.org/10.1039/d4mh00552j

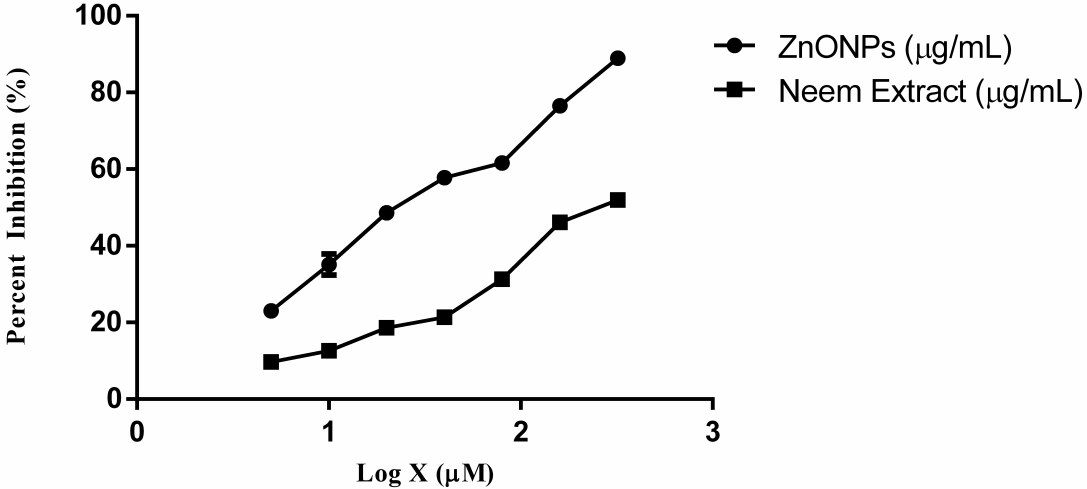
40. Setyawati, M. I., Tay, C. Y., & Leong, D. T. (2013). Effect of zinc oxide nanomaterials-induced oxidative stress on the p53 pathway. Biomaterials, 34(38): 10133–10142. https://doi.org/10.1016/j.biomaterials.2013.09.024

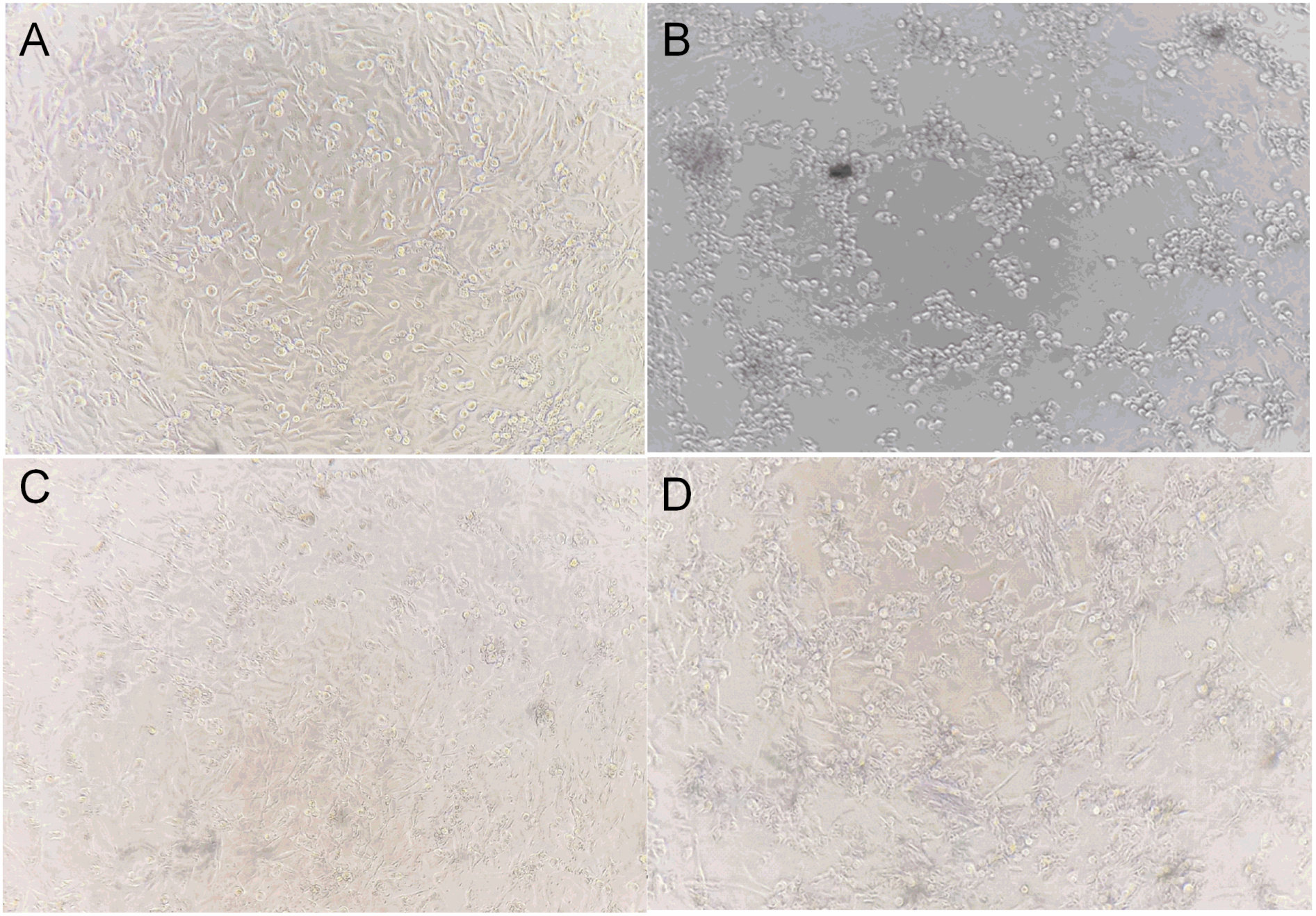
41. Bader Almutairi, Ali, D., Yaseen, K. N., Alothman, N. S., NoufAlyami, HanoufAlmukhlafi, Saad Alakhtani, & Saud Alarifi. (2021). Mechanisms of Apoptotic Cell Death by Stainless Steel Nanoparticle Through Reactive Oxygen Species and Caspase-3 Activities on Human Liver Cells. Frontiers in Molecular Biosciences, 8. https://doi.org/10.3389/fmolb.2021.729590

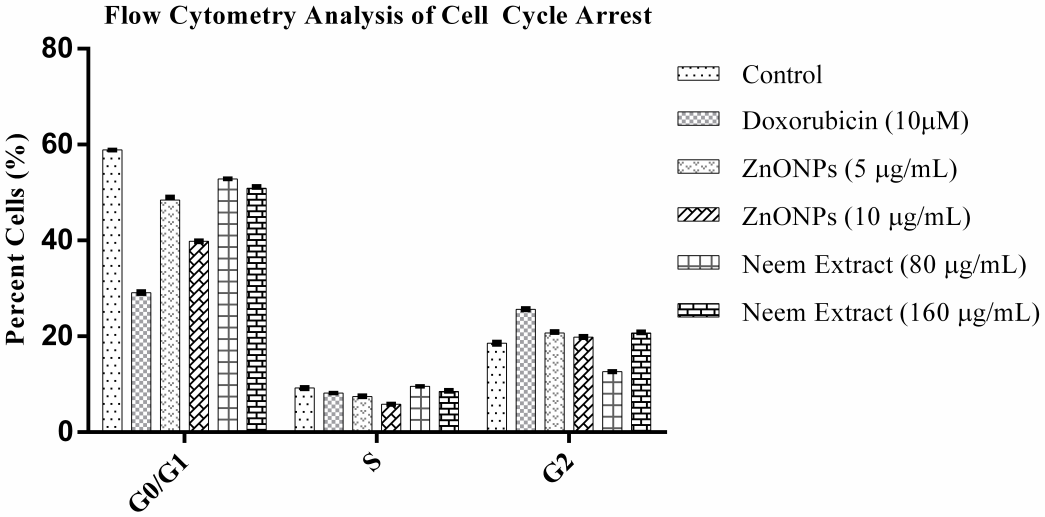
42. Taylor RC, Cullen SP, Martin SJ. (2008). Apoptosis: controlled demolition at the cellular level. Nature Reviews Molecular Cell Biology. 9(3):231–241. https://doi:10.1038/nrm2312

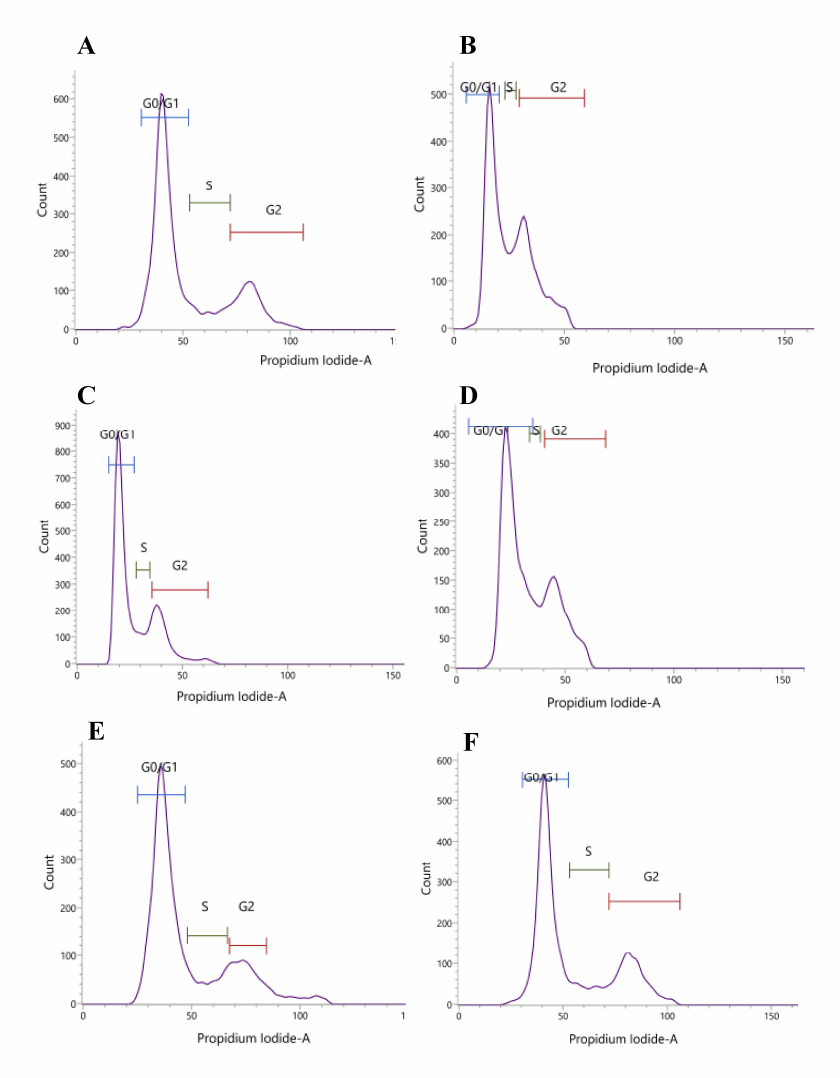
43. Rufini A, Tucci P, Celardo I, Melino G (2013). Senescence and aging: the critical roles of p53. Oncogene. 32(43):5129–5143. https://doi:10.1038/onc.2012.640

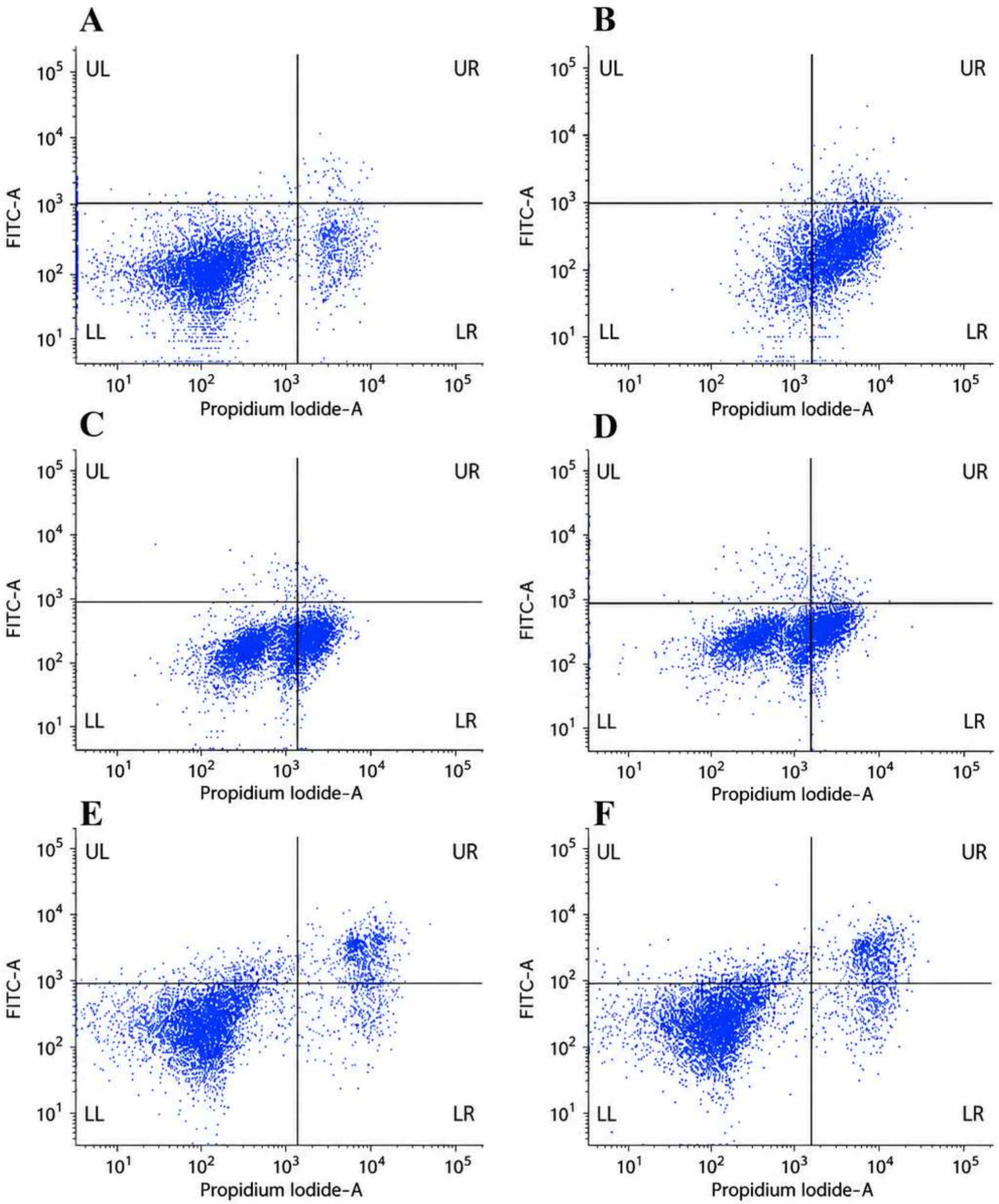

Doxorubicin Standard
Percent Inhibition (%)
100
80
60
40
20
0
0.0
0.5
1.0
1.5
2.0
2.5
Log X (μM)

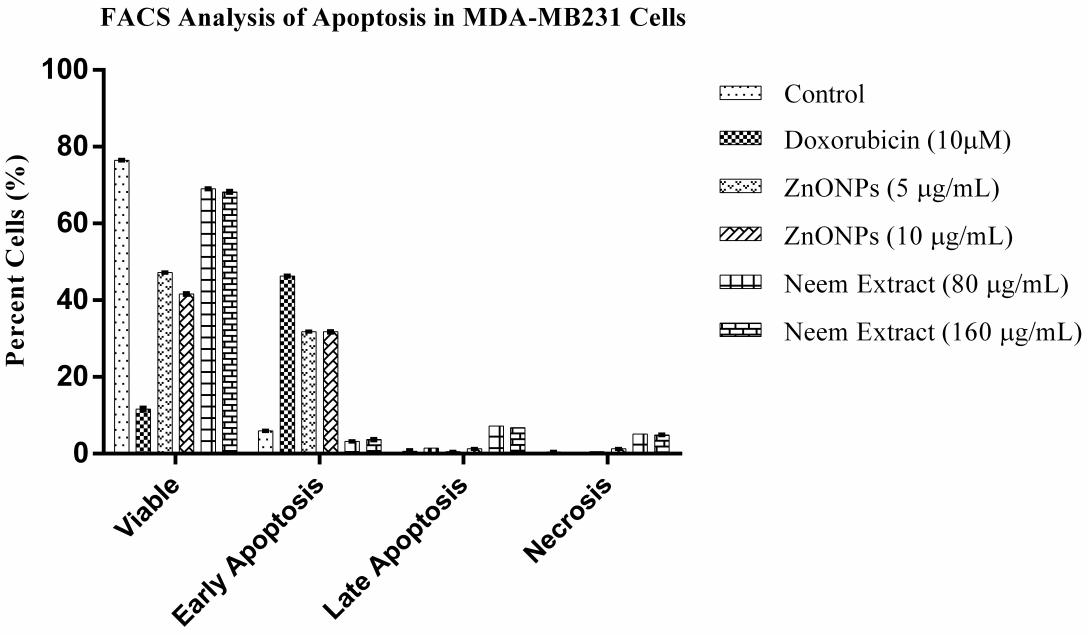

100
80
60
40
20
0
Percent Inhibition (%)
0
1
2
3
Log X (μM)
ZnONPs (μg/mL)
Neem Extract (μg/mL)

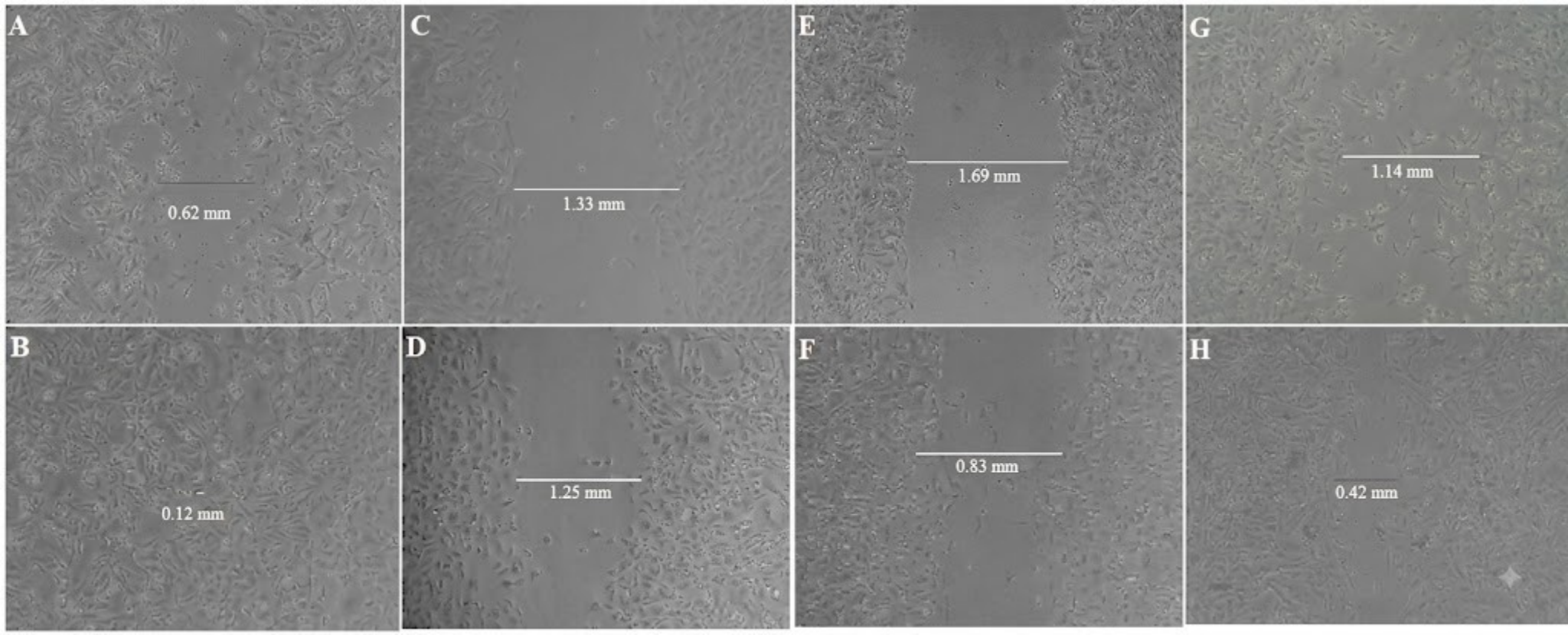

A
B
C
D

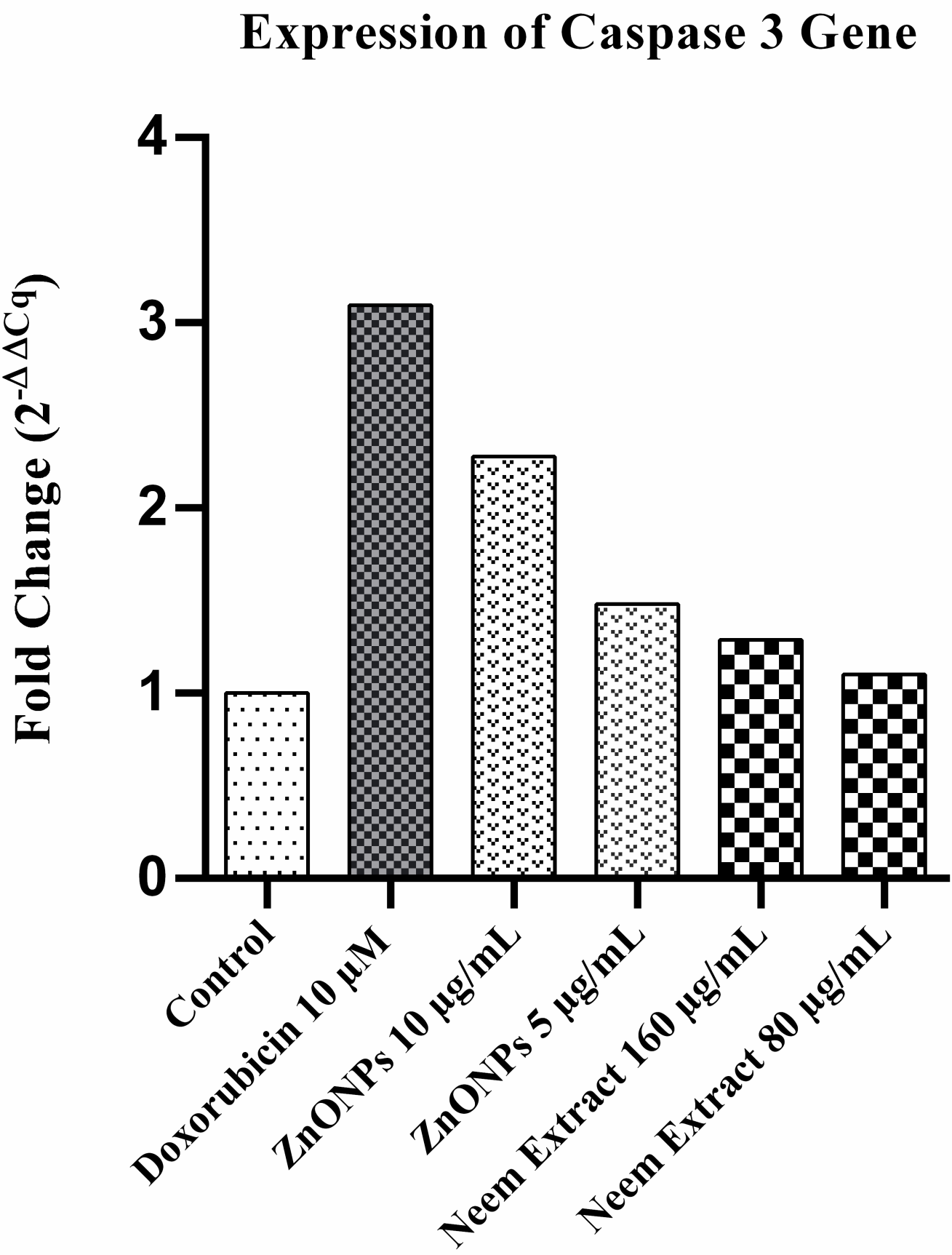

Flow Cytometry Analysis of Cell Cycle Arrest
Percent Cells (%)
80
60
40
20
0
G0/G1
S
G2
Control
Doxorubicin (10μM)
ZnONPs (5 μg/mL)
ZnONPs (10 μg/mL)
Neem Extract (80 μg/mL)
Neem Extract (160 μg/mL)

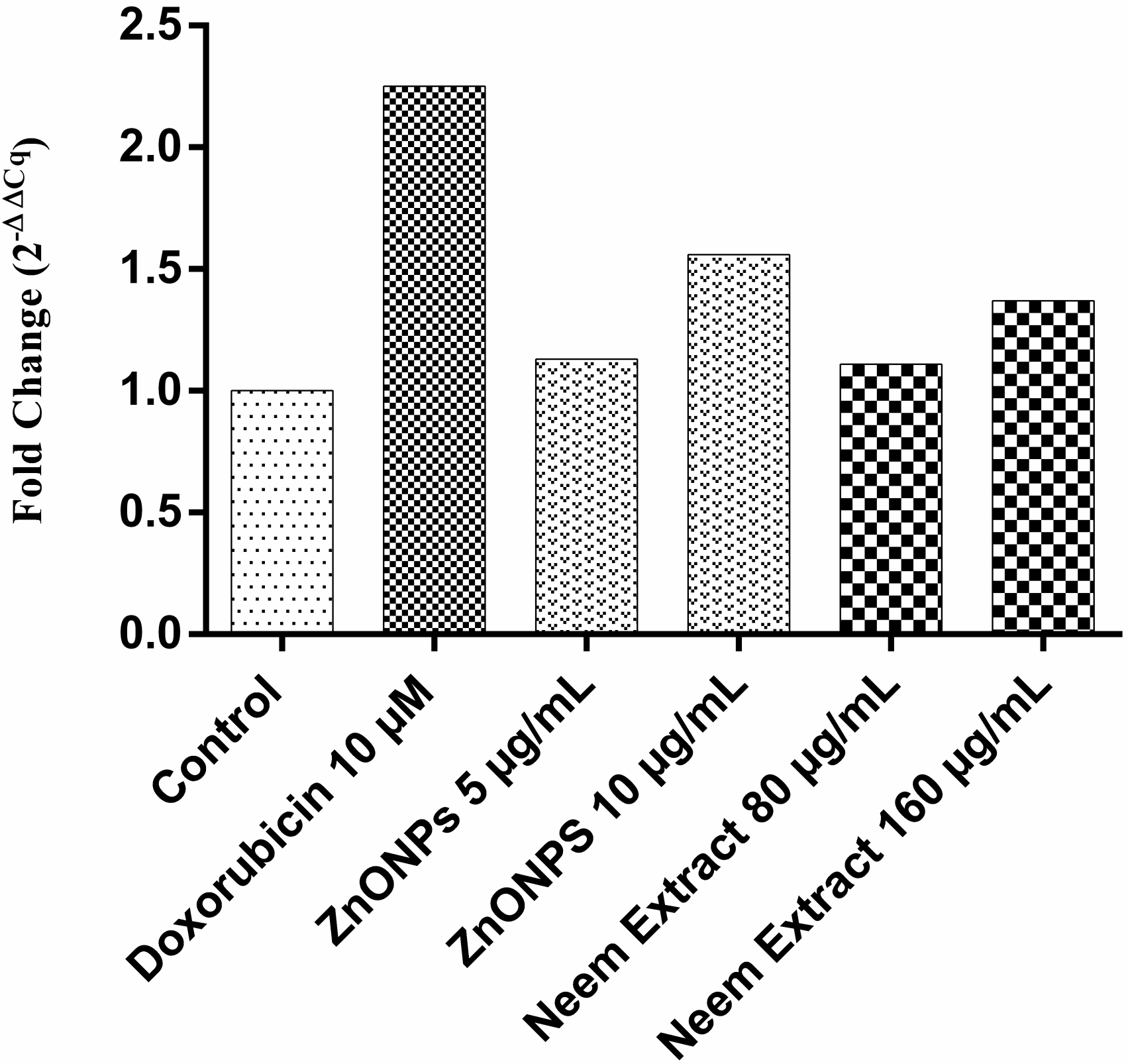

A
G0/G1
S
G2
Count
Propidium Iodide-A
B
G0/G1
S
G2
Count
Propidium Iodide-A
C
G0/G1
S
G2
Count
Propidium Iodide-A
D
G0/G1
S
G2
Count
Propidium Iodide-A
E
G0/G1
S
G2
Count
Propidium Iodide-A
F
G0/G1
S
G2
Count
Propidium Iodide-A


A
B
C
D
E
F
UL
UR
LL
LR
FITC-A
Propidium Iodide-A
10^1
10^2
10^3
10^4
10^5


FACS Analysis of Apoptosis in MDA-MB231 Cells
Percent Cells (%)
100
80
60
40
20
0
Viable
Early Apoptosis
Late Apoptosis
Necrosis
Control
Doxorubicin (10μM)
ZnONPs (5 μg/mL)
ZnONPs (10 μg/mL)
Neem Extract (80 μg/mL)
Neem Extract (160 μg/mL)


A
0.62 mm
C
1.33 mm
E
1.69 mm
G
1.14 mm
B
0.12 mm
D
1.25 mm
F
0.83 mm
H
0.42 mm


Expression of Caspase 3 Gene
Fold Change ($2^{-\Delta\Delta Cq}$)
4
3
2
1
0
Control
Doxorubicin 10 µM
ZnONPs 10 µg/mL
ZnONPs 5 µg/mL
Neem Extract 160 µg/mL
Neem Extract 80 µg/mL


Expression of p53 Gene
Fold Change ($2^{-\Delta\Delta C_q}$)
2.5
2.0
1.5
1.0
0.5
0.0
Control
Doxorubicin 10 µM
ZnONPs 5 µg/mL
ZnONPS 10 µg/mL
Neem Extract 80 µg/mL
Neem Extract 160 µg/mL

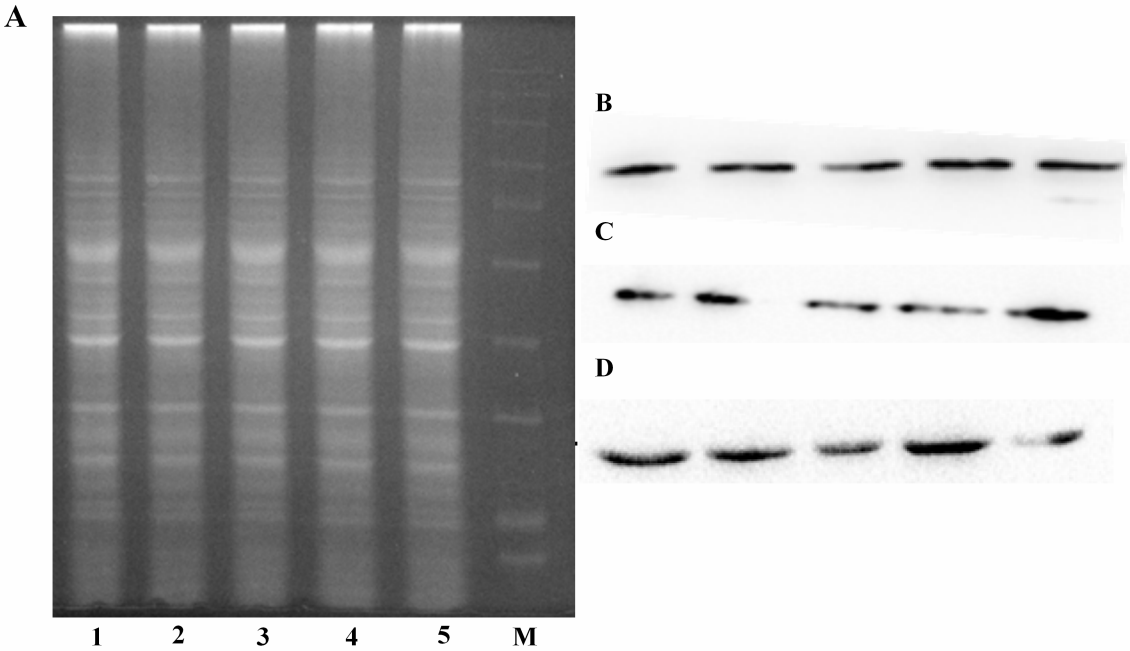

A
B
C
D
1
2
3
4
5
M

Table 1: Effect of Neem extract, ZnONPs, and doxorubicin on wound closure and cell migration inhibition in the in vitro cell migration (scratch) assay.

Treatment	Concentration	Initial wound width, 0 h (mm)	Wound width, 24 h (mm)	Wound width, 48 h (mm)	Wound closure, 24 h (%)	Wound closure, 48 h (%)	Migration inhibition, 24 h (%)	Migration inhibition, 48 h (%)
Untreated control	—	1.98	0.62	0.12	68.59	93.94	—	—
Doxorubicin	10 µM	2.01	1.83	1.25	9.15	37.81	86.66	59.75
ZnONPs	10 µg/mL	1.99	1.69	0.83	15.33	58.49	77.65	37.74
Neem extract	160 µg/mL	2.00	1.14	0.42	43.00	78.90	37.31	16.01

Table 2: Relative Normalized Expression of Caspase 3 Gene

Treatment Group	Caspase 3	GAPDH	ΔCq	ΔΔCq	Fold change 2^-ΔΔCq
Control	27.27	20.84	6.44	0.00	1.00
Doxorubicin (10 µg/ml)	250.	20.25	4.75	-1.63	3.095
ZnONPs (10µg/ml)	25.33	20.09	5.25	-1.19	2.28
ZnONPs (5µg/ml)	25.63	19.77	5.87	-0.57	1.48
Plant Extract (160 µg/ml)	26.06	19.99	6.07	-0.36	1.29
Plant Extract (80 µg/ml)	25.95	19.65	6.30	-0.13	1.10

Cq - Quantification Cycle

Table 3: Relative Normalized Expression of p53 Gene

Treatment Group	p53	GAPDH	ΔCq	ΔΔCq	Fold change 2^-ΔΔCq
Control	26.45	20.84	5.62	0.00	1.00
Doxorubicin (10 µg/ml)	24.70	20.25	4.45	-1.17	2.25
ZnONPs (10µg/ml)	25.06	20.09	4.98	-0.64	1.56
ZnONPs (5µg/ml)	25.20	19.77	5.44	-0.18	1.13

Plant Extract (160 µg/ml)	25.15	19.99	5.16	-0.45	1.37
Plant Extract (80 µg/ml)	25.12	19.65	5.47	-0.15	1.11

Cq - Quantification Cycle